Hindawi
Mobile Information Systems
Volume 2022, Article ID 3498258, 9 pages
https://doi.org/10.1155/2022/3498258

Research Article

Fuzzy Control Path Planning of Soccer Robot Relying on Quantum Genetic Algorithm

Xiaoming Yang

School of Information Engineering and Automation Kunming University of Science and Technology, Kunming 650051, Yunnan, China

Correspondence should be addressed to Xiaoming Yang; kmyxm@kust.edu.cn

Received 9 March 2022; Revised 28 April 2022; Accepted 11 May 2022; Published 10 June 2022

Academic Editor: Muhammad Muzammal

When planning the soccer robot path at present, a two-dimensional map is used mainly to optimize the path of the soccer robot's operating field. However, because the two-dimensional robot is selected, which can only utilize the data of plane about a specific environment, the data information of the mobile soccer robot cannot be gathered, impacting greatly the completion of the plan of the robot path. The path planning of the soccer robot is conducted using the quantum genetic algorithm so that the problem can be dealt with. On the premise that there is a lack of full consideration of the accurate motion path between the two points, the inertia weight is dynamically adjusted to overcome the disadvantage of premature convergence of the traditional quantum group algorithm, which can make the weight of the quantum genetic algorithm controllable with adaptability so that the problem of the extremely slow convergence speed of a single quantum in the quantum group and the high group dispersion can be solved. Furthermore, the selected quantum genetic algorithm can realize the real-time update of the soccer robot's position, effectively increase the trajectory change of the particle swarm movement, and to a certain extent effectively increase the search ability and convergence effect of the particle swarm in the global scope, so as to ensure that this algorithm can be more effective than the traditional path planning algorithm in terms of global search ability and convergence speed in the path planning of the soccer robot and has a higher use value.

1. Introduction

Soccer robot is one of the hotspots in the current international robotics research field [1–3]. Soccer robot is a mobile machine that simulates athletes for training. Therefore, the best, fastest, and collision-free path planning to efficiently avoid obstacles in the moving process becomes the bottleneck of manual control in the movement process [4–7]. At present, domestic and foreign researchers have effectively combined particle swarm algorithm, neural network algorithm, quantum theory, genetic algorithm, and other algorithms and used them in large-scale robot path planning. The theoretical research status of the soccer robot path is slowly turning to the path of group optimization calculation. Its quantum genetic algorithm is a new type of group optimization calculation method. The features of the objective function are not standardized with this method, the excellent optimization function cannot be completed easily along with it, and it has gradually become an important goal of robot intelligent control optimization research in China and other countries. The use of the quantum genetic algorithm to calculate soccer robots makes planning easier and the calculation method simpler, but the search function has a large dependence on parameters, which will cause some problems of small results. Regarding how to improve the results of quantum particle groups to be more accurate and comprehensive, many researchers have reformed and optimized quantum group calculation methods. Since the computer technology and Internet technology have developed continuously, people's research on robots has become multifaceted and intelligent. In many occasions of daily life and industrial processing and production, people maximize the use of robots in order to obtain maximum economic benefits. In this circumstance, traditional methods for soccer robot path planning will not be able to meet the functional requirements. Therefore, it is more important to apply the

quantum genetic algorithm to fuzzy control path planning for soccer robot to navigate its motion in indoor environment.

The quantum group computing method mostly relies on the global value to transmit information, which is faster and more accurate than other computing methods. The disadvantage is that it will end earlier. Regarding this shortcoming, this paper finds the main algorithm of the study, the quantum genetic algorithm, which uses the single quantum optimization progress and the overall dispersed dynamic motion proportion, so that the inertia proportion contains control characteristics and adaptive characteristics. This algorithm can quickly improve the convergence progress of the calculation, maintain the characteristics of different groups, enhance the comprehensive search advantage of the calculation, and so on. Finally, according to the calculation methods proposed in this paper, it is applied to the trajectory planning of soccer robots. Through comparison with the common calculation methods, the analysis of the experimental results is performed, the result of which shows that the quantum genetic algorithm proposed in this paper is more effective than the traditional one in the path planning of the soccer robot [8–15].

2. Quantum Genetic Algorithm

If the optimization of the genetic algorithm is realized in accordance with the characteristics of the quantum particle swarm, the path planning is not required to convert the speed in the search process. Therefore, the calculation process of the quantum genetic algorithm is simpler, and fewer reference objects exist for comparison, which can be easily managed. The comparison with traditional algorithms shows that both the convergence speed and search ability of the quantum genetic algorithm are more significant.

After the optimization of the quantum genetic algorithm, the calculation formula is as follows:

$$X_{i,j}(t+1) = p_{i,j}(t) \pm \alpha \cdot \left| M_j(t) X_{i,j}(t) \right| \cdot \mathrm{In}\left(\frac{1}{u}\right). \tag{1}$$

$$P_{i.j} = \phi \cdot P\mathrm{best}_{i,j}(t) + (1-\phi) \cdot G\mathrm{best}(t), \quad (i = 1, 2 \ldots N,\ j = 1, 2, \ldots M). \tag{2}$$

$$m\mathrm{best} = \left(M_1(t), M_2(t), \ldots, M_D(t) = \left\{ \frac{1}{N}\sum_{i=1}^{N} p\mathrm{best}_{i,1}(t), \frac{1}{N}\sum_{i=1}^{N} p\mathrm{best}_{i,2}(t), \ldots, \frac{1}{N}\sum_{i=1}^{N} p\mathrm{best}_{i,1}(t) \right\}. \tag{3}$$

According to the above expression, the ith quantum particle can be represented by $X_i = \{X_{i,1}(t), X_{i,2}(t), \ldots X_{i,D}(t)\}$ expression at t; the optimal position of each particle is expressed by $p\mathrm{best}_i = \{p\mathrm{best}_{i,1}(t), p\mathrm{best}_{i,2}(t), \ldots p\mathrm{best}_{i,D}(t)\}$; the optimal position of the whole process is represented by $G\mathrm{best} = \{G\mathrm{best}_1(t), G\mathrm{best}_2(t), \ldots, G\mathrm{best}_D(t)\}$; the mean value corresponding to the optimal position is represented by $\mathrm{mest} = \{M_1(t), M_2(t), \ldots M_D(t)\}$; the position and number of the quantum particle group and the number of iterations are represented by D, N, and M; $\phi = c_1 r_1/(c_1 r_1 + c_2 r_2)$; α represents the expansion and contraction amount; c_1, c_2 represent the convergence factor; and r_1, r_2 represent the average number of particles dispersed.

In the process of genetic algorithm optimization calculation, it is very important to realize the effective control of its parameters. According to the evolutionary formulas (1) and (3), the convergence characteristics of the quantum genetic algorithm calculation method can be improved. According to formula (2) of the quantum $p_i(t+1)$, it can be converted into the following formula:

$$p_{i,j}(t+1) = G\mathrm{best}_{i,j}(t) + \phi\left(p\mathrm{best}_{i,j}(t) - G\mathrm{best}_{i,j}(t)\right). \tag{4}$$

Based on (1) and (4), the conversion quantum $p_i(t+1)$ and overall optimal relation $G\mathrm{best}(t)$ are specially related to the itch gap between the quantum optimal relation $p\mathrm{best}(t)$ at that time, and the relationship that exists between $X_i(t+1)$ and the corresponding quantum mean is related to the error value at position $X_{(t)}$.

When selecting parameters, the calculation method in this paper uses the individual quantum optimization speed and the inertia proportion of the overall separation, so that the inertia proportion contains the self-adaptive aggregation degree, which can effectively avoid the problem of premature convergence of genetic particles in the process of global search, and at the same time, a random selection algorithm can be used to ensure the quantum motion to the optimal position. In order to effectively ensure the diversification and stability of the particle swarm motion, the convergence capacity of the genetic algorithm can be effectively promoted based on the enhancement of the global search capacity of the particle swarm.

Definition 1. The optimization speed of the quantum particle swarm can use the function Fitness Gbest(t) to represent the overall motion characteristics of the particle swarm, and use the function Fitness $P_i(t)$ to represent the optimal characteristics of the current particle swarm, and then the expression for particle swarm optimization can be obtained as follows:

$$ip_i(t) = \frac{\mathrm{Fitness}(G\mathrm{best}(t))}{\mathrm{Fitness}(G\mathrm{best}_i(t))}. \tag{5}$$

When the minimum value of the particle swarm satisfies $0 < ip \le 1$, if the ip value is reduced, the speed of this movement will gradually increase. If $ip = 1$, the quantum genetic algorithm can be used to obtain the optimal value.

Definition 2. The dispersion degree of the particle swarm can ensure that the quantum particle swarm used can find the optimal gap $\partial_p(t)$ represented by $\partial_p(t) = \{\partial_{p1}(P\mathrm{best}_{i,1}(t)), \partial_{p2}\ (P\mathrm{best}_{i,2}(t)), \cdots \partial_{P\,D}(P\mathrm{best}_{i,D}(t))\}$, and using this expression, the quantum swarm dispersion can be obtained as follows:

$$gs_t(t) = \left\{gs_{i,1}(t), gs_{i,2}(t), \ldots gs_{i,D}(t)\right\} = \left\{\frac{\partial_{p1}\left(P\text{best}_{i,1}(t)\right)}{\partial_{X1}\left(X_{i,1}(t)\right)}, \frac{\partial_{p2}\left(P\text{best}_{i,2}(t)\right)}{\partial_{X2}\left(X_{i,2}(t)\right)}, \ldots, \frac{\partial_{p\ D}\left(P\text{best}_{i,D}(t)\right)}{\partial_{X\ D}\left(X_{i,D}(t)\right)}\right\}. \quad (6)$$

According to the above expression, *gs* can represent the progress of particle discrete optimization. If the value of *gs* changes, the quantum discrete optimization progress will be accelerated, and due to the difference in the size of the quantum population, the speed will be reduced. If $gs = 1$ is satisfied, then the obtained optimal value *Pbest* is inconsistent with the current value, which will cause the value of *gs* to change continuously.

3. Fuzzy Control Path Planning of Soccer Robot

Aiming at solving the problems of traditional genetic algorithm in robot path planning, neuro-fuzzy controller is used to adjust the solution to the local minimum point problem in quantum genetic algorithm, so as to improve the real-time performance and effectiveness of robot dynamic planning in the process of fuzzy control. The fuzzy control variable can be represented by a ternary array $(r_1, r_2, r_3) r_1 < r_2 < r_3$, and its membership function is as follows:

$$\mu(x) = \begin{cases} \dfrac{x - r_1}{r_2 - r_1}, \\ \dfrac{x - r_3}{r_2 - r_3}, \\ 0. \end{cases} \quad (7)$$

Assuming the fuzzy control path planning $\alpha = (a_1, a_2, a_3)$ and $\beta = (b_1, b_2, b_3)$ according to the expansion principle of fuzzy control retrieval number addition and scalar multiplication, we can obtain the following:

$$\mu_{\overline{\alpha}+\overline{\beta}}(z) = \sup\left\{\min\left\{\mu_{\overline{\alpha}}(x), \mu_{\overline{\beta}}(y)\right\} | z = x + y\right\} = \begin{cases} \dfrac{z - (a_1 + b_1)}{(a_2 + b_2) - (a_1 + b_1)} \\ \dfrac{z - (a_3 + b_3)}{(a_2 + b_2) - (a_3 + b_3)}. \\ 0 \end{cases} \quad (8)$$

That is, the sum of the fuzzy control path planning is still the fuzzy control path planning, and

$$\overline{\alpha} + \overline{\beta} = (a_1 + b_1, a_2 + b_2, a_3 + b_3). \quad (9)$$

Based on $\mu_{\lambda\overline{\alpha}}(z) = \sup\{\mu_{\overline{\alpha}}(x) | z = \lambda x\}$, we can obtain the following:

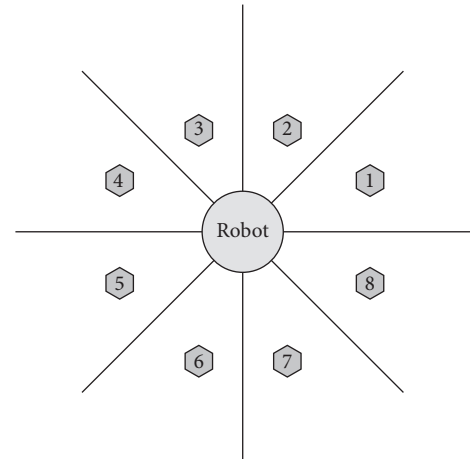

Figure 1: Soccer robot system structure.

$$\lambda\overline{\alpha} = \begin{cases} (\lambda a_1, \lambda a_2, \lambda a_3), \lambda \geq 0 \\ (\lambda a_4, \lambda a_3, \lambda a_2), \lambda < 0 \end{cases}. \quad (10)$$

Assuming $\overline{\alpha}_i = (a_{i1}, a_{i2}, a_{i3})$, $i = 1, 2, \ldots, m$, be the fuzzy control path planning, we obtain the nonnegative linear combination of $\overline{\alpha}_i$ and the fuzzy control path planning:

$$\sum_{i=1}^{m} \lambda_i \overline{\alpha}_i, \lambda_i \geq 0. \quad (11)$$

It is still fuzzy control path planning, and

$$\sum_{i=1}^{m} \lambda_i \overline{\alpha_i} = \left(\sum_{i=1}^{m} \lambda_i a_{i1}, \sum_{i=1}^{m} \lambda_i a_{i3}\right). \quad (12)$$

As for the fuzzy control path planning environment, the opportunity is understood as the possibility that the establishment of the constraints is conducted. The fuzzy control path planning is made use of to effectively solve the optimization problem of the path planning parameters of the robot.

The double circular arc curve equation is used to calculate the dynamic change of the motion curve based on the fuzzy control parameter α during the motion of the soccer robot. The parameters α and β are used as the variables of the fuzzy control (Figure 1).

In the quantum swarm algorithm, quantum represents the motion path of the soccer robot. In this paper, *N* motion trajectories are set, and the quantum dimension *D* represents the number of paths from the starting point to the end point. The process of the path planning of the soccer robot can be represented as the planning process of obtaining the optimal angle value under each path planning.

Due to the movement scene of the soccer robot, this paper selects the grid algorithm to optimize the constructed robot path planning model. The selected grid method selects the motion path of the soccer robot for grids with the same size. Both the polar coordinates and rectangular coordinates can be used to display the motion scene of soccer robot for path planning. The length of polar coordinate represents the straight-line distance

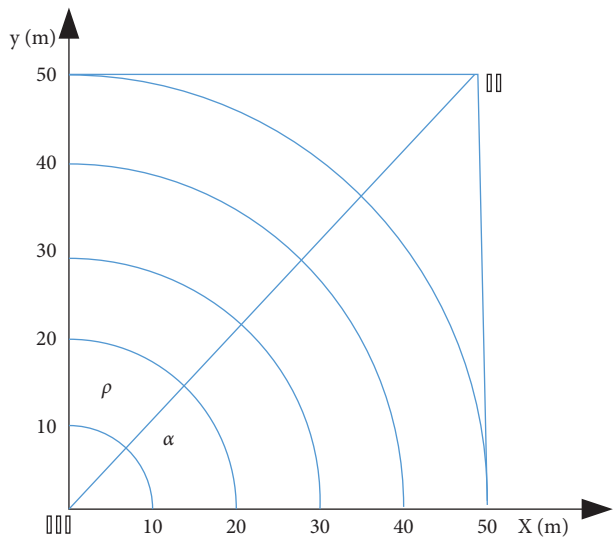

Figure 2: Soccer robot movement distance in polar coordinates and rectangular coordinates.

from the initial motion position to the stop position of the soccer robot, and the angle represents the motion trajectory of the soccer robot within the range of motion. The grid specifications need to be set reasonably according to the motion range of the soccer robot and the specifications of the obstacles. Both the polar coordinates and rectangular coordinates are combined to represent the detection of the relationship as shown in Figure 2.

Suppose that the parameter values of the quantum particle swarm are set: D represents the quantum motion dimension; M represents the maximum number of iterations of the particle; N represents the quantum swarm; learning factors are C_1 and C_2; and the expansion-contraction coefficient is α. The dimension of the quantum group motion can be calculated as follows:

$$\mathrm{D} \approx \frac{\mathrm{distance}(\mathrm{path})}{\mathrm{length}_{\mathrm{robot}}}. \tag{13}$$

In the expression, distance path is used to calculate the straight-line distance from the initial point to the end point, and $\mathrm{length}_{\mathrm{robot}}$ represents the height of the soccer robot.

The establishment straight-line distance from the initial point to the end point of the soccer robot is the determining factor for the length of the polar coordinates. The range of detection angle used is $[0, \pi/2]$; then, the expression can be used as follows:

$$\begin{cases} \alpha_{\max} = \alpha_{\mathrm{top}}, \alpha_{\min} = \alpha_{\mathrm{down}}, \rho \mathrm{L} \le \mathrm{L}_{\mathrm{target}}, \\ \alpha_{\max} = \alpha_{\mathrm{top}}, \alpha_{\min} = \alpha_{\mathrm{down}}, \rho \mathrm{L} > \mathrm{L}_{\mathrm{target}}. \end{cases} \tag{14}$$

In the above formula, $\beta = \arccos(L_{\mathrm{target}}/\rho_i)$, and α_{top} and α_{down}, respectively, represent the maximum and minimum values that the soccer robot can reach in the range of motion; the constraints that need to be satisfied are as follows:

$$\rho_L = \frac{\sqrt{\left(x_j - x_0\right)^2 - \left(y_j - y_0\right)^2}}{D}. \tag{15}$$

The distribution of the quantum group settings is relatively uniform, and the search position and movement speed are represented as follows:

$$\alpha_{\mathrm{i,j}} = \mathrm{rand} * \left(\alpha_{\mathrm{top}} - \alpha_{\mathrm{down}}\right) + \alpha_{\mathrm{down}}. \tag{16}$$

The calculation process of the fuzzy control path planning algorithm proposed in this paper is shown in Figure 3, according to which $G = (S, E)$ represents the grid map of the robot in the plane, S represents the grid corresponding to the motion position of the soccer robot, and E represents the reachable boundary of the motion position. The function $a_{dj}(s)$ represents the raster grid within the motion area. If the first grid $s_{\mathrm{start}} \in S$ and the target grid of soccer robot motion satisfies $\{s_{\mathrm{goal}} \in S\}$, the fuzzy control path planning algorithm used in this paper can be applied to the function $g(s)$ for calculating the consumption of s from the initial position to each motion position, and the optimal motion path can be obtained.

$$g(s) = \begin{cases} 0, & \text{if } s = s_{\mathrm{start}}, \\ \min_{s' \in P_{\mathrm{red}}(s)} \left(g\left(s'\right) + c\left(s', s\right)\right), & \text{otherwise.} \end{cases} \tag{17}$$

The real-time position of the soccer robot on the field is represented by $h(s)$, and the initial speed is set to 0. If the grid where the robot is located can pass smoothly, the obtained data information cannot be determined for the soccer robot. If $g(s_{\mathrm{start}}) = 0$ is satisfied, then S can be represented by CLOSED when it is not necessary to complete this barrier setting. The full grid of robot motion is represented by $s \in a_{dj}(s_{\mathrm{start}})$ and can be represented in this way by the function $g(s)$ and the value $h(s, s_{\mathrm{goal}})$. In the detection, if the no grid s is apparent in the CLOSED sequence, then in the motion sequence, the OPEN sequence can use the $k(s)$ function to search according to the grid where the soccer robot is set.

$$k(s) = g(s) + h\left(s, s_{\mathrm{goal}}\right). \tag{18}$$

Before formulating the plan of the path of the soccer robot on the field, a model of the field environment needs to be built, mainly to ensure that the soccer robot is familiar with the field environment. By dividing the field position where the soccer robot is located into several grids, the abstract description is carried out according to the grid of the field.

The total length of the field is represented by m, and the width is represented by n. Taking the upper left corner of the field as the origin, and setting the grid coordinates of the upper left corner as $(0, 0)$, the Cartesian coordinate system of the soccer robot movement is constructed. If the boundary of the field is represented by a, the size of a can be regarded as a soccer robot motion cell grid, and the number of grids of the field can be represented by the grid number $\mathrm{ceil}(m/a)$ of different columns, where ceil represents the upward movement direction of the soccer robot.

In the fuzzy control path planning, the motion path can be converted according to the algorithm, and the mapping

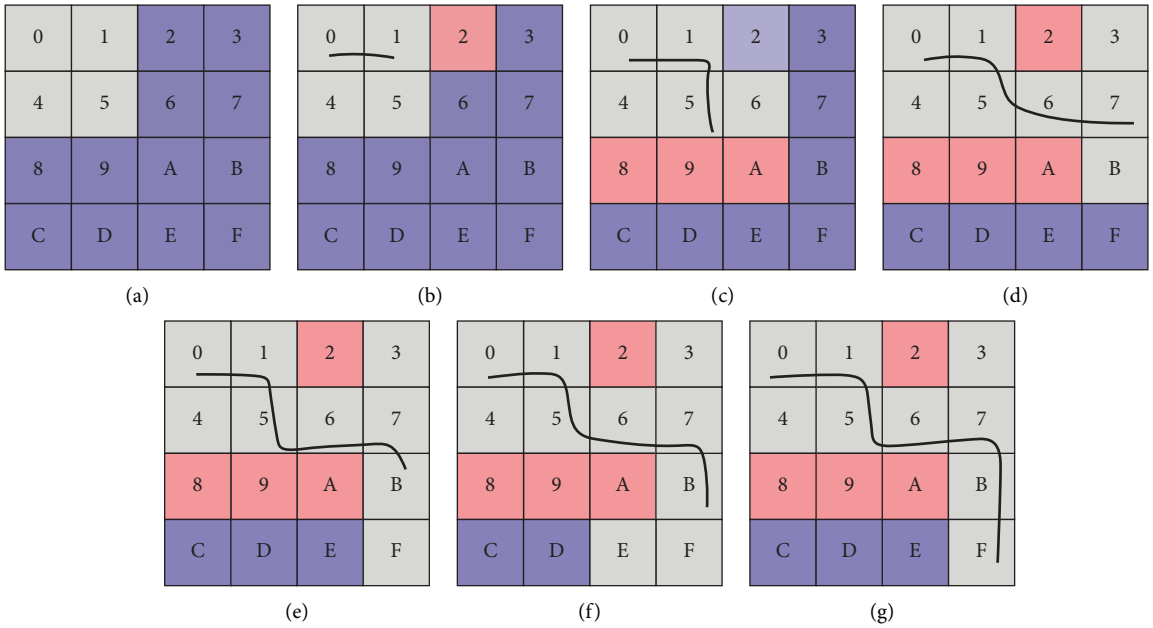

Figure 3: Example diagram of fuzzy control path planning.

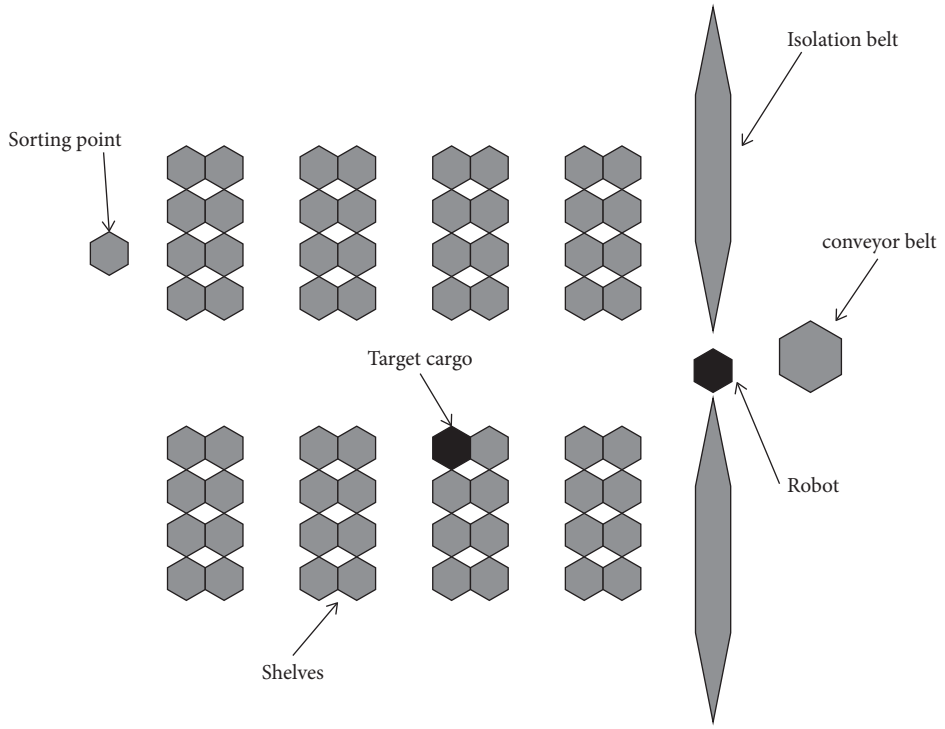

Figure 4: Partial schematic diagram of simulated field sports.

relationship between the soccer robot and the field can be represented as follows:

$$\text{bianhao} = (x-1) \times \text{ceil}\left(\frac{m}{a}\right) + y. \tag{19}$$

Figure 4 is a schematic diagram of simulating the local movement of the soccer robot on the field.

By setting the controller parameters according to Table 1, the layer-by-layer control steps of the system are calculated as follows:

(1) Fuzzification layer: The input variables of the fuzzy control system (the displacement between the robot and the obstacle and the relative movement between the two to form the angle θ, the relative velocity ΔV)

Table 1: Parameter settings of adaptive neuro-fuzzy controller.

ANFIS1 variable	Input		Output
	D_2	θ	K_2
Domain	(0, 2)	$(-\pi, \pi)$	(1, 100)
Fuzzy subset number	4	8	32
Membership function	Bell-shaped membership function		
Parameter training	Hybrid method		
ANFIS2 variable	Input		Output
	θ	ΔV	β
Domain	$(-\pi, \pi)$	(−1, 1)	(1, 100)
Fuzzy subset number	8	7	56
Membership function	Bell-shaped membership function		
Parameter training	Hybrid method		

can be fuzzified, and the node i has an output function:

$$\begin{aligned} O_i^1 &= \mu_{A_i}(D_2), \quad i = 1, 2, 3, 4, \\ O_i^1 &= \mu_{B_{i-4}}(\theta), \quad i = 5, \ldots, 12, \\ O_i^1 &= \mu_{c_{i-12}}(\Delta V), \quad i = 13, \ldots, 19. \end{aligned} \tag{20}$$

In the formula, the fuzzy sets A_i, B_i, and C_i are planned as shown in Table 1, and the D_2 with the universe of discourse of (0, 2), θ with the universe of discourse of $(-\pi, \pi)$, and the ΔV with the universe of discourse of (−1, 1) are divided into (ZD, SD, MD, FD), (NH, NB, NM, NS, Z, PS, PM, PB), and (NB, NM, NS, Z, PS, PM, PB), respectively. O_i^1 is the membership function value of A_i and B_i. Selecting (μAi), ($\mu Bi - 4$), and ($\mu Ci - 12$) are used as the membership function to calculate the corresponding maximum value of 1 and minimum value of 0. Then,

$$\begin{aligned} \mu_{A_i}(D_2) &= \frac{1}{1 + \left[\left(D_2 - q_i / m_i \right)^2 \right]^{p_i}}, \\ \mu_{B_{i=4}}(\theta) &= \frac{1}{1 + \left[\left(\theta - q_{i-4} / m_{i-4} \right)^2 \right]^{p_{i-4}}}, \\ \mu_{C_{i-12}}(\Delta V) &= \frac{1}{1 + \left[\left(\Delta V - q_{i-12} / m_{i-12} \right)^2 \right]^{p_{i-12}}}. \end{aligned} \tag{21}$$

In the formula, m, p, and q are the antecedent parameters, and the shape of the membership function changes with the change of these three parameters.

(2) Operation layer (fuzzy inference layer): Perform operation on the input signal. The output of each node represents the credibility of the rule, and its output is as shown in the following formulas:

$$O_i^2 = \omega_i = \mu_A(D_2) \times \mu_B(\theta), \quad i = 1, \ldots, 32, \tag{22}$$

$$O_i^2 = \omega_i = \mu_A(\theta) \times \mu_C(\Delta V), \quad i = 33, \ldots, 88. \tag{23}$$

The control rules represented by (22) and (23) are listed in Tables 2 and 3.

Table 2: ANFIS1 fuzzy rule set.

D_2	θ							
	NH	NB	NM	NS	Z	PS	PM	PB
ZD	NA	SA	SA	MA	BA	MA	SA	SA
SD	NA	NA	NA	SA	MA	MA	SA	NA
MD	NA	NA	NA	SA	MA	SA	NA	NA
FD	NA	NA	SA	SA	SA	SA	NA	NA

Table 3: ANFIS2 fuzzy rule set.

Δv	θ							
	NH	NB	NM	NS	Z	PS	PM	PB
NBV	BA	MA	SA	NA	NA	NA	SA	MA
NMV	MA	SA	NA	NA	NA	NA	SA	SA
NSV	SA	NA	NA	NA	NA	NA	NA	NA
ZV	NA	NA	NA	NA	NA	NA	NA	NA
PSV	NA	NA	NA	SA	SA	SA	NA	NA
PMV	NA	NA	NA	SA	MA	SA	NA	NA
PBV	NA	NA	NA	MA	BA	MA	NA	NA

Note. Z: zero; S: small; M: middle; B: large; D: distance; N: negative; H: huge; P: positive.

(3) Normalization layer: The ith node calculates the normalized credibility of the ith rule:

$$\begin{aligned} O_i^3 &= \overline{\omega_i} = \frac{\omega_i}{\sum_1^{32} \omega_i}, \quad i = 1, \ldots, 32, \\ O_i^3 &= \overline{\omega_i} = \frac{\omega_i}{\sum_{33}^{88} \omega_i}, \quad i = 33, \ldots, 88. \end{aligned} \tag{24}$$

(4) Conclusion layer: The output contained in the ith node is as follows:

$$\begin{aligned} O_i^3 &= \overline{\omega_i} f_i = \overline{\omega_i}(xD_2 + y\theta + z), \quad i = 1, \ldots, 32, \\ O_i^4 &= \overline{\omega_i} f_i = \overline{\omega_i}(x\Delta V + y\theta + z), \quad i = 33, \ldots, 88. \end{aligned} \tag{25}$$

In the formula, $\overline{\omega_i}$ is the output of the third layer, and x, y, and z are the consequent parameters.

(5) Deblurring layer: This layer calculates the total output:

Table 4: Mechanism characteristic values related to the wheeled soccer robot.

Item	Parameter
Mass of the robot	2.3 kg
Mass of one driving wheel of the robot	0.28 kg
Geometric center distance from the robot center of mass to the driving wheel	0.065 m
Rotary inertia of robot	0.1 kg·m^2
Rotary inertia of driving wheel	0.0022 kg·m^2
Spacing of driving wheel	0.3 m
Radius of driving wheel	0.068 m
Pulse number of motor turnover	16
Frequency multiplication of control chip	2
Pulse counting cycle of encoder	0.005 s
Reduction ratio of the reducer	131
Time interval during which the robot sends the pulse code to the upper computer through the serial port	0.3 s

$$O_i^5 = K_2 = \sum_{i=1}^{32} \overline{\omega_i} f_i, \quad i = 1, \ldots, 32,$$
$$O_i^5 = \beta = \sum_{i=32}^{88} \overline{\omega_i} f_i, \quad i = 33, \ldots, 88. \tag{26}$$

Among them, the universes of discourse of K2 and β are both (1, 100).

4. Result and Analysis of Simulation

In practical application, the two-wheeled soccer robot is taken as the research target in order to test the effect of the algorithm in this paper. Among control parameters, the set parameter values of the wheeled soccer robot are shown in Table 4. The number of experiments is set to 100, and the path planning results obtained from the test are shown in Figure 5.

According to the experimental results in Figure 5, the result of the soccer robot path planning according to the quantum genetic algorithm is better than that of the traditional genetic algorithm. The length of the planned path is 4.0253 m upon the measurement, while the motion path length of the soccer robot under the traditional genetic algorithm is 4.3813 m. The main reason is that the traditional one is prone to plunge into the local optimum in the process of searching for the path, but the optimal path can be obtained by applying the quantum genetic algorithm to the global search of the soccer robot.

Based on the test results of experiments in Figures 6 and 7, the soccer robot can obtain the local optimal value after 149 iterations under both the traditional genetic algorithm and the quantum one. However, the quantum genetic algorithm used in this paper can be far beyond the local optimal value after 200 iterations and search for the global optimal path after about 250 iterative adjustments, but the soccer robot is still involved in the local optimal path under the traditional genetic algorithm. According to the above-mentioned explanation, the quantum genetic algorithm

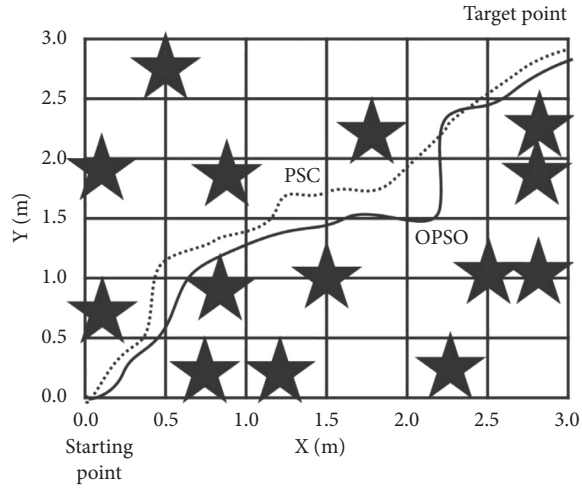

Figure 5: Comparison of optimal path results between the traditional genetic algorithm and the quantum one.

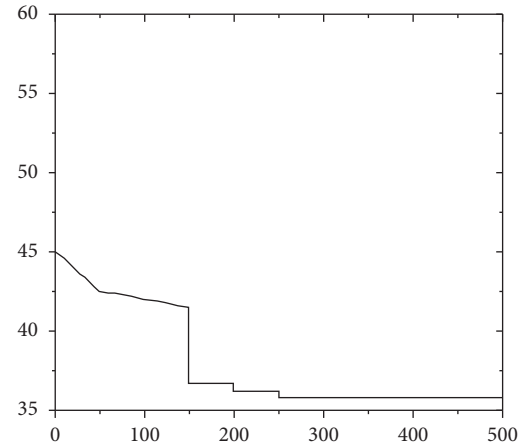

Figure 6: Convergence result of the traditional genetic algorithm.

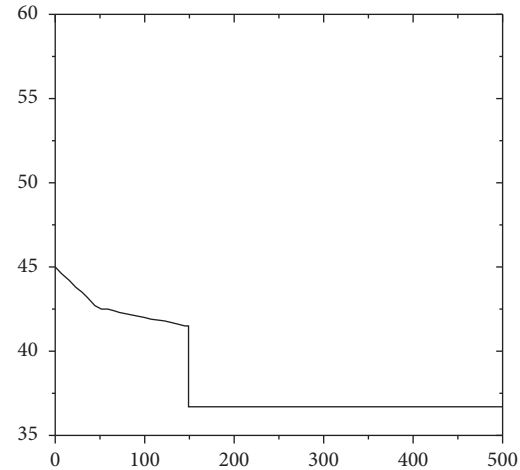

Figure 7: Convergence result of the quantum genetic algorithm.

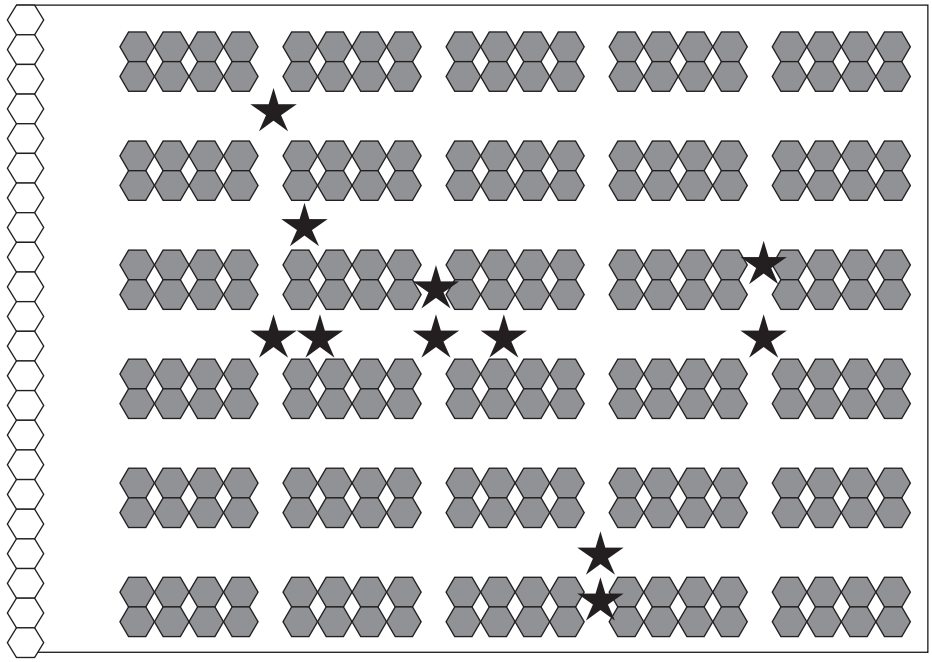

Figure 8: Rasterized warehousing environment.

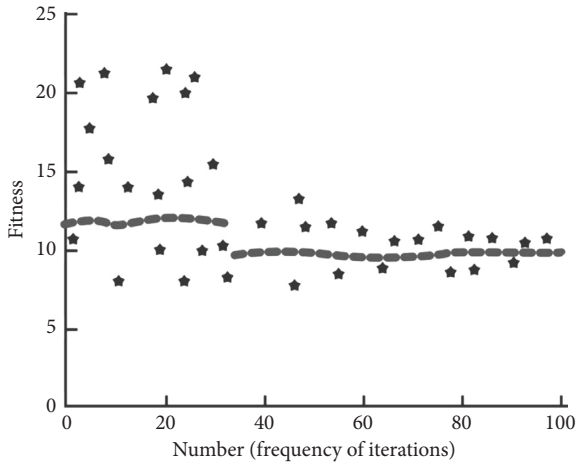

Figure 9: Comparison between optimal path length and average path length under different iterations.

proposed in this paper is better than the traditional genetic algorithm in the global convergence speed.

The B_i application is on the basis of selecting an automated stereo field and building a rasterized environment of field as shown in Figure 8.

The warehousing environment after being rasterized is as shown in Figure 8, which is composed of a total of 23 parts in the size classification station on the left side of the field. Following the path formed by the next-door protective casing, only one soccer robot can pass through all paths, that is, a single passenger ticket. A lot of selection work by sifting is completed in the field by soccer robot at the speed of 1 m/s.

The performance of quantum genetic algorithm significantly affects the result of fuzzy control path planning of soccer robot, which is testified in this section. Figure 9 shows the changing process of the individual fitness of each generation according to the number of evolutionary generation when using the quantum genetic algorithm. Figure 9 shows the concentrated points representing the mean fitness values of each generation, and the points which are comparatively dispersed nearby represent the optimal fitness values of each generation, wherein the optimal fitness values of each generation match the mean fitness value of the generation.

The experimental results in Figure 9 show that the quantum genetic algorithm used in this paper can effectively be used to improve the convergence speed of the soccer robot and most quantum groups can quickly find the global optimal solution. In the initial process of the quantum genetic algorithm, if the individual expected value difference is too large, the particle swarm can be quickly optimized during the processing. In the later particle iteration process, if the particle swarm is similar to the optimal solution, the obtained optimal path is closer to the real situation and avoids the emergence of local optimal solutions.

5. Conclusion

During the process of soccer robot path planning, choosing a reasonable and scientific path has gradually become the key goal of current research. In this paper, quantum genetic algorithm and adaptive neuro-fuzzy artificial potential field are used to plan and study the fuzzy control route of soccer robot and plan the soccer robot's mobile path. The selected plane grid map can realize the calculation of the movement range of the soccer robot and can test the collision phenomenon in the robot movement process, so as to avoid the deadlock phenomenon of the robot. The trap prediction mechanism is added, so that the robot can overcome the limitation of the sensor measurement range to a certain

extent and can conduct relevant analysis of spatial feasibility more quickly. The purpose is to provide support for the generation of fuzzy rules when dealing with the establishment of a fuzzy system and to facilitate the planning of the optimal path of the soccer robot. The robot simulation results show that the soccer robot can effectively assist people in heavy and repetitive mechanical work on the field, and using it in the field can effectively improve the management level of the field and save labor costs. The experimental results verify that the algorithm in this paper can perform optimal path planning.

Data Availability

The data used to support the findings of this study are available from the author upon request.

Conflicts of Interest

The author declares no conflicts of interest.

References

[1] J. Guo, C. Li, and S. Guo, "A novel step optimal path planning algorithm for the spherical mobile robot based on fuzzy control," *IEEE Access*, vol. 8, no. 3, pp. 1394–1405, 2020.

[2] B. Sun, D. Zhu, and S. X. Yang, "An optimized fuzzy control algorithm for three-dimensional AUV path planning," *International Journal of Fuzzy Systems*, vol. 20, no. 2, pp. 597–610, 2018.

[3] H. Tourajizadeh and O. Gholami, "Optimal control and path planning of a 3PRS robot using indirect variation algorithm," *Robotica*, vol. 38, no. 5, pp. 1–22, 2019.

[4] A. A. Sori, A. Ebrahimnejad, and H. Motameni, "Elite artificial bees' colony algorithm to solve robot's fuzzy constrained routing problem," *Computational Intelligence*, vol. 36, no. 11, pp. 1–10, 2019.

[5] C. Yang, Y. Jiang, J. Na, Z. Li, L. Cheng, and C.-Y. Su, "Finite-time convergence adaptive fuzzy control for dual-arm robot with unknown kinematics and dynamics," *IEEE Transactions on Fuzzy Systems*, vol. 27, no. 3, pp. 574–588, 2019.

[6] M. A. H. Ali and M. Mailah, "Path planning and control of mobile robot in road environments using sensor fusion and active force control," *IEEE Transactions on Vehicular Technology*, vol. 1, no. 3, pp. 1–7, 2019.

[7] G. Bai, Y. Meng, L. Liu, W. Luo, Q. Gu, and K. Li, "Anti-sideslip path tracking of wheeled mobile robots based on fuzzy model predictive control," *Electronics Letters*, vol. 56, no. 10, pp. 490–493, 2020.

[8] C. F. Juang and T. B. Bui, "Reinforcement neural fuzzy surrogate-assisted multiobjective evolutionary fuzzy systems with robot learning control application," *IEEE Transactions on Fuzzy Systems*, vol. 28, no. 3, pp. 434–446, 2019.

[9] Y. Fan, Y. An, W. Wang, and C. Yang, "T-S fuzzy adaptive control based on small gain approach for an uncertain robot manipulators," *International Journal of Fuzzy Systems*, vol. 22, no. 3, pp. 930–942, 2020.

[10] T. Abut and S. Soyguder, "Real-time control and application with self-tuning PID-type fuzzy adaptive controller of an inverted pendulum," *Industrial Robot: The International Journal of Robotics Research and Application*, vol. 46, no. 1, pp. 159–170, 2019.

[11] J. N. Pires and A. S. Azar, "Advances in robotics for additive/hybrid manufacturing: robot control, speech interface and path planning (#literatiawards winner 2019)," *Industrial Robot*, vol. 45, no. 3, pp. 9–17, 2018.

[12] P. Quillen and K. Subbarao, "Minimum control effort–based path planning and nonlinear guidance for autonomous mobile robots," *International Journal of Advanced Robotic Systems*, vol. 15, no. 6, pp. 68–76, 2018.

[13] Z. C. Duan, J. P. Li, J. Qin et al., "Demonstration of compiled Shor's quantum factoring algorithm using a quantum dot single-photon source," *Optics Express*, vol. 28, no. 13, pp. 1–7, 2020.

[14] A. Moradnouri, M. Vakilian, A. Hekmati, and M. Fardmanesh, "Optimal design of flux diverter using genetic algorithm for axial short circuit force reduction in HTS transformers," *IEEE Transactions on Applied Superconductivity*, vol. 30, no. 1, pp. 1–8, 2020.

[15] J. Tan, Z. Liu, and H. Chen, "Entanglement in phase estimation algorithm and quantum counting algorithm," *International Journal of Theoretical Physics*, vol. 59, no. 4, pp. 105–112, 2020.